JPET Fast Forward. Published on August 7, 2008 as DOI: 10.1124/jpet.108.140327

JPET#140327

Dynamics of Aβ Turnover and Deposition in Different APP Transgenic Mouse Models Following Gamma-Secretase Inhibition

Abramowski, Dorothee, Karl-Heinz Wiederhold, Ulrich Furrer, Anne-Lise Jaton, Anton Neuenschwander, Marie-Josephine Runser, Simone Danner, Julia Reichwald, Domenico Ammaturo, Dieter Staab, Markus Stoeckli, Heinrich Rueeger, Ulf Neumann, Matthias Staufenbiel

Novartis Institutes for BioMedical Research, 4002 Basel, Switzerland

JPET Fast Forward. Published on August 7, 2008 as DOI: 10.1124/jpet.108.140327
This article has not been copyedited and formatted. The final version may differ from this version.

Running title: Dynamics of Aβ Turnover in APP Transgenic Mice

Corresponding author: Matthias Staufenbiel

Novartis Pharma AG

4002 Basel, Switzerland

Tel: +41613249642

Fax +41613245524

E-mail: Matthias.Staufenbiel@novartis.com

Number of text pages: 36

Number of tables: 1

Number of figures: 9

Number of references: 40

Number of words in *Abstract*: 248

Number of words in *Introduction*: 602

Number of words in *Discussion*: 1596

Abbreviations: Aβ Amyloid β; AD Alzheimer's Disease; APP Amyloid precursor protein; BACE β-site APP cleaving enzyme; CSF Cerebrospinal fluid; CTF C-terminal fragment; ELISA Enzyme-linked immunosorbent assay; GFAP Glial fibrillary acidic protein; MALDI-TOF Matrix assisted laser desorption/ionization-time of flight mass spectrometry; PS Presenilin; TBS Tris buffered saline

Recommended section assignment: Neuropharmacology

JPET Fast Forward. Published on August 7, 2008 as DOI: 10.1124/jpet.108.140327
This article has not been copyedited and formatted. The final version may differ from this version.

Abstract

Human β-amyloid precursor protein (APP) transgenic mice are commonly used to test potential therapeutics for Alzheimer's disease (AD). We have characterized the dynamics of β-amyloid (Aβ) generation and deposition following γ-secretase inhibition with compound LY-411575. Kinetic studies in pre-plaque mice distinguished a detergent soluble Aβ pool in brain with rapid turnover (half-lives for Aβ40 and Aβ42 were 0.7 and 1.7 h) and a much more stable, less soluble pool. Aβ in cerebrospinal fluid (CSF) reflected the changes in the soluble brain Aβ pool, while plasma Aβ turned over more rapidly. In brain APP C-terminal fragments (CTF) accumulated differentially. The half-lives for γ-secretase degradation were estimated as 0.4 and 0.1 h for C99 and C83, respectively. Three different APP transgenic lines responded very similarly to γ-secretase inhibition regardless of the familial Alzheimer's disease mutations in APP. Amyloid deposition started with Aβ42 while Aβ38 and Aβ40 continued to turn over. Chronic γ-secretase inhibition lowered amyloid plaque formation to a different degree in different brain regions of the same mice. The extent was inversely related to the initial amyloid load in the region analyzed. No evidence for plaque removal below baseline was obtained. γ-secretase inhibition led to a redistribution of intracellular Aβ and an elevation of CTFs in neuronal fibers. In CSF Aβ showed a similar turnover as in pre-plaque animals demonstrating its suitability as marker of newly generated, soluble Aβ in plaque-bearing brain. This study supports the use of APP transgenic mice as translational models to characterize Aβ lowering therapeutics.

JPET Fast Forward. Published on August 7, 2008 as DOI: 10.1124/jpet.108.140327
This article has not been copyedited and formatted. The final version may differ from this version.

Introduction

Deposits of the Aβ peptide known as amyloid plaques are one of the defining pathological hallmarks of Alzheimer's disease and aggregated Aβ species are considered to play a key role in disease pathogenesis (Hardy and Selkoe, 2002). Generation of Aβ from the membrane-bound β-amyloid precursor protein (APP) involves consecutive cleavage by the β-secretase, BACE1 and the γ-secretase complex (Wolfe, 2006). BACE catalyzes the cleavage at the N-terminus of Aβ, releasing a soluble form of APP (sAPPβ), and leaving a C-terminal fragment (C99) in the membrane. C99 is then processed by γ-secretase, which possibly involves three successive cleavage steps (Zhao et al., 2005) finally yielding a set of Aβ peptides heterogeneous at the C-terminus, with the most abundant ends at positions 40, 42 and 38. The other product of this cleavage is the APP intracellular domain thought to be a regulator of gene expression (Wolfe, 2006). The γ-secretase is a complex composed of presenilins (PS1 or PS2), nicastrin, presenilin enhancer-2 (PEN-2) and APH-1. Considerable evidence suggests that the presenilins contain the active site of this intramembrane aspartyl protease (Wolfe, 2006). A large number of presenilin mutations are associated with familial AD (Tandon and Fraser, 2002). They usually shift the Aβ generation to the longer Aβ42 isoform as demonstrated in cellular and transgenic models (Citron et al., 1997) as well as in AD patients (Scheuner et al., 1996). γ-secretase was shown to also cleave a number of other type I transmembrane proteins (Selkoe and Kopan, 2003), the best characterized one being Notch, an important regulator of cell fate. Accordingly, mice deficient in PS1 (Wong et al., 1997) or nicastrin (Li et al., 2003) are not viable, while PS2-KO mice survive and lack an overt phenotype (Donoviel et al., 1999).

Because of its pivotal role in Aβ generation, γ-secretase has been a target of drug development and several substances have been described to inhibit γ-secretase in vitro (Shearman et al., 2000; Dovey et al., 2001), in rats (Best et al., 2005), in guinea pigs (Anderson et al., 2005) and in several APP transgenic mouse models of Alzheimer's disease (Dovey et al., 2001; Cirrito et al., 2003; Lanz et al., 2004; Wong et al., 2004; Anderson et al., 2005; Barten et al., 2005; Best et al., 2005; Churcher et al., 2006; Best et al., 2007). Inhibition of γ-secretase in rodents resulted in a substantial reduction of Aβ in brain and

cerebrospinal fluid (CSF) within a few hours after substance application. In several in vivo models Aβ reduction by either γ-secretase inhibition or conditional presenilin knockout was accompanied by a beneficial effect on cognitive function (Comery et al., 2005; Dash et al., 2005; Saura et al., 2005). However, severe side effects concerning lymphatic and intestinal cell differentiation have been observed for γ-secretase inhibitors seemingly due to inhibition of Notch cleavage (Searfoss et al., 2003; Wong et al., 2004). Application to humans has been described for one γ-secretase inhibitor only, which showed reduction of Aβ in plasma, but not in CSF (Siemers et al., 2007).

In this study we used the γ-secretase inhibitor LY-411575 (May et al., 2001) to characterize the dynamics of Aβ in brain, CSF and plasma in several APP transgenic mouse models before onset of amyloid plaque formation. The corresponding changes in the γ-secretase substrates, the APP C-terminal fragments, were analyzed in comparison. Subfractionation of brain was used to distinguish Aβ populations with different turnover. We also analyzed the effect of chronic reduction of Aβ production in a preventive as well as a therapeutic paradigm, i.e. in pre-plaque and plaque-bearing mice. Our study describes key characteristics of Aβ generation and deposition in APP transgenic mice.

Methods

Experimental animals- The transgenic mouse lines used express human APP751 under the control of the murine Thy1-promoter, resulting in neuron specific expression. APP23 mice (Sturchler-Pierrat et al., 1997) express APP with the KM670/671NL “Swedish” mutation. In APP24 mice the “Swedish” double mutation was combined with the “London” mutation V717I. APP51/16 mice express wildtype APP (Herzig et al., 2004). APP23 and APP51/16 overexpress human APP about 7 and 10 times over endogenous APP. Mostly compact amyloid plaques start appearing at the ages of about 6 and 12-15 months, respectively. In APP24 mice, overexpression of human APP is about 3.5-fold. Mostly diffuse amyloid plaques start appearing at 8 months of age. The mice were on a C57BL/6 background and hemizygous for the transgene. All animal experiments were in compliance with protocols approved by the Swiss Animal Care and Use Committees.

JPET Fast Forward. Published on August 7, 2008 as DOI: 10.1124/jpet.108.140327
This article has not been copyedited and formatted. The final version may differ from this version.

Substance application and brain concentration- The γ-secretase inhibitor N^2-[(2S)-2-(3,5-difluoro-phenyl)-2-hydroxyethanoyl]-N^1-[(7S)-5-methyl-6-oxo-6,7-dihydro-5H-dibenzo[b,d]azepin-7-yl]-L-alaninamide (LY-411575; for chemical structure see Wong et al., 2004) was used. Mice received vehicle alone (0.25% methylcellulose in water) or 1-10 mg/kg LY-411575 suspended in vehicle solution by oral gavage at 20 ml/kg. The following compound concentrations [mean±SD in nM] were determined in brain after treatment of male mice with 10 mg/kg LY-411575: 0.5 h, 111±45; 1 h, 83±8; 2 h, 52±6; 4 h, 33±4; 6 h, below limit of quantification. For comparison, the cellular IC_{50} value of LY-411575 is about 0.1 nM (Wong et al., 2004 and our unpublished results with APP23 and APP51/16 primary neurons).

Mouse sacrifice and tissue sampling- CSF was sampled from the cisterna magna under anesthesia with 3% isoflurane. In most cases 3-10 µl of CSF could be obtained. Mice were decapitated and EDTA-plasma was prepared from the blood. In experiments with chronic substance treatment, one brain hemisphere was fixed by immersion in 4% formaldehyde solution. For biochemical investigation, forebrain was prepared from the second hemisphere by removal of olfactory bulb and hindbrain, frozen on dry ice and stored at -80°C until used. After chronic treatment of APP24 mice, the olfactory bulb and the pons/medulla oblongata from one brain hemisphere were also isolated and frozen on dry ice.

Homogenization of brain tissue- Brain regions were weighed and homogenized by sonication in 10 volumes of Tris-buffered saline (TBS; 20 mM Tris-HCl pH 7.6, 137 mM sodium chloride, protease inhibitor cocktail Complete, Roche Diagnostics, Mannheim, Germany).

Determination of APP and its metabolites- Aβ was quantified using different methods (Western blotting, quantitative MALDI-TOF, ELISA and an electrochemiluminescence linked immunoassay). To obtain standards for the quantifications, dilution series of the analytes [synthetic Aβ1-38/40/42 peptides (Bachem, Torrance, CA and r-Peptide, Bogart, GA), recombinant sAPPα and sAPPβ (Meso Scale Discovery, Gaithersburg, MD), APP (in transgenic mouse brain homogenates)] were prepared in non-transgenic mouse brain extract or plasma. The presence of non-transgenic CSF had no influence on ELISA calibration curves from synthetic Aβ standards. Therefore standards for determination of CSF Aβ

were prepared without addition of CSF from non-transgenic mice.

Immunoprecipitation of Aβ- For immunoprecipitation of Aβ from brain tissue, homogenates were extracted with 1% sodium dodecyl sulfate at 95°C for 3 min, diluted with 9 volumes of TBS and cleared by centrifugation. Aβ peptides were immunoprecipitated using the monoclonal antibody β1 reacting with an epitope near the amino-terminus of Aβ (Schrader-Fischer and Paganetti, 1996) and protein G coated magnetic beads (Dynal Biotech, Hamburg, Germany). Antibody β1 does not recognize rodent Aβ under the conditions used. For immunoprecipitation of Aβ from plasma, antibody β1 covalently coupled to sepharose beads was used.

Dephosphorylation of APP C-terminal fragments- Forebrain homogenates were supplemented with 1% Nonidet P-40 (Fluka, Buchs, Switzerland), 50 mM HEPES (pH 7.5), 0.1 mM Na_2EDTA, 5 mM dithiothreitol, 0.01% Brij 35, 3 mM $MnCl_2$ and were incubated with E.coli λ-phosphatase (New England Biolabs, Ipswich, MA, 400 units per mg forebrain) at 30°C for 1 hour. The reaction was stopped by addition of SDS sample buffer.

Gel electrophoresis and Western blotting- For detection of Aβ, immunoprecipitates, CSF or brain homogenates were separated on 10% Tris-bicine acrylamide gels with 8 M urea as described (Klafki et al., 1996). C-terminal APP fragments were separated on 10% or 13% Tris-bicine acrylamide gels without urea and were detected with rabbit antiserum APP-C8 raised against the carboxy-terminal amino acids of APP (Schrader-Fischer and Paganetti, 1996). Transgene derived APP and Aβ were detected with the human-specific monoclonal antibody 6E10 (Signet, Dedham, MA). Total APP was detected with antibody 22C11 (Roche Molecular Biochemicals, Rotkreuz, Switzerland). The bands obtained on films were quantified using the software MCID (version M7 elite, InterFocus Imaging Ltd, Cambridge, England). Some of the CSF samples analyzed by Western blotting (Figure 5) were slightly contaminated with blood, and globin comigrated with Aβ1-38 on the gel, which precluded quantification of the Aβ1-38 band. For detection of presenilin 1, forebrain homogenates from 5 animals per group were separated on 13% Tris-glycine acrylamide gels and PS1 CTFs were detected on Western blots with antibody R28 (Baumann et al., 1997) directed against the large cytoplasmic loop of presenilin 1.

JPET Fast Forward. Published on August 7, 2008 as DOI: 10.1124/jpet.108.140327
This article has not been copyedited and formatted. The final version may differ from this version.

Aβ quantification by MALDI-TOF- Aβ immunoprecipitated with antibody β1 and protein G coated magnetic beads as described above was eluted with a acetonitrile/water/formic acid solution (50:40:10, v/v/v) saturated with α-cyano-4-hydroxy-cinnamic acid. As internal standard, 10 pM bovine insulin was added. Samples were loaded on a MALDI-TOF target plate (Applied Biosystems, Framingham, MA) and dried at ambient temperature. Mass spectra were acquired in the mass range 3000 to 6000 Dalton using an Applied Biosystems Voyager-DE sSTR TOF mass spectrometer. Aβ peptides were located on the spectra by identifying the most prominent peak in a region of ±5 Dalton of the calculated mass of each peptide. For quantification, the peak height was used, as the area under the curve yielded less reliable results, when irrelevant peaks were present adjacently.

Aβ quantification by ELISA- For determination of total Aβ40 or Aβ42, forebrain homogenates were extracted for 15 min at 4°C with 70% formic acid. The extracts were neutralized by addition of 19 volumes 1 M Tris-base and centrifuged for 15 min at 20 000xg. For pre-plaque mice, the supernatant was directly applied to ELISA plates (IBL Human Amyloid β (1-40) JP27713 or (1-42) JP27711 Assay, IBL, Hamburg, Germany and Innotest β-Amyloid 1-42 #80177 Assay, Innogenetics, Gent, Belgium). When forebrains with high plaque load were analyzed, the extracts were further diluted in 70% formic acid, neutralized and diluted in sample dilution buffer from the ELISA kit, as necessary to achieve an Aβ concentration within the standard curve. For analysis of TBS soluble Aβ, forebrain homogenates were centrifuged at 100 000xg for 15 min. For Triton X-100 soluble Aβ, Triton X-100 was added to the forebrain homogenate (final concentration 1%) and samples were extracted on ice for 15 min before centrifugation at 100 000xg. Samples were mixed every 5 min. The supernatants were diluted (total dilution 1:80) with sample dilution buffer from the ELISA kit (see above), as undiluted extracts caused high background and a low signal to noise ratio. For determination of Aβ in CSF, the IBL Human Amyloid β (1-40) and the Innotest β-Amyloid 1-42 assays were used.

Aβ quantification by electrochemoluminescence-linked immunoassay- MSD 96-Well MULTI-ARRAY Human (6E10) Abeta 40 or Abeta 42 Ultra-Sensitive Kits were used (Meso Scale Discovery, Gaithersburg, MD). For Aβ40 determination in plasma samples were cleared by centrifugation (1 min,

JPET Fast Forward. Published on August 7, 2008 as DOI: 10.1124/jpet.108.140327
This article has not been copyedited and formatted. The final version may differ from this version.

20 000xg), mixed with an equal volume of 3% Blocker A solution included in the assay kit and further processed according to the manufacturers instructions. Signals were measured on a SECTOR™ Imager 6000 reader (Meso Scale Discovery). Triton-X-100 soluble Aβ was prepared as described for ELISAs and diluted to a final dilution of 1:100 with 3 % Blocker A. This method was also used to verify the Aβ reductions in some experiments and the Aβ concentrations by direct comparison of all pre-plaque control groups.

Determination of sAPPα and sAPPβ by electrochemoluminescence-linked immunoassay- Forebrain homogenates were extracted with 1% Triton X-100 on ice for 15 min. Samples were centrifuged (15 min, 4°C, 20 000xg). The supernatants were further diluted with 1% Triton X-100 in TBS (total dilution 1:2000), loaded on a MS6000 sAPPalpha/sAPPbeta multiplex plate (Meso Scale Discovery) and further processed as described for Aβ.

Estimation of Aβ and CTF half-life and production rate- The time course of Aβ concentrations after γ-secretase inhibition is described by the equation

$$[A\beta]_t = [A\beta]_0 * e^{(-k*t)} + \text{offset} \quad \text{(Eq. 1)}$$

where $[A\beta]_t$ and $[A\beta]_0$ are the concentrations of Aβ at time t and start (in vehicle treated mice), respectively. k is the first-order rate constant of Aβ removal, and offset is the amount of Aβ not affected by treatment. Data pairs (t, $[A\beta]_t$) were fitted to the above equation to determine k (Origin 7.5 software, Origin lab corporation, Northampton, MA). The half-life was calculated using

$$t_{½} = \ln 2/k \quad \text{(Eq. 2).}$$

Under steady-state conditions, which can be assumed to exist in pre-plaque mice, the rate of production, k' of Aβ equals its rate of clearance. It can be calculated from

$$k' = k*([A\beta]_0 - \text{offset}) \quad \text{(Eq. 3).}$$

An independent estimate of Aβ production rates was obtained from average Aβ loads measured in 11 and 18.3 months old APP23 mice with the formula:

JPET Fast Forward. Published on August 7, 2008 as DOI: 10.1124/jpet.108.140327
This article has not been copyedited and formatted. The final version may differ from this version.

$$k' = \frac{[A\beta]_{18.3\ mo} - [A\beta]_{11\ mo}}{18.3\ mo - 11\ mo} \quad \text{(Eq. 4).}$$

Half-lives of C99 and C83 were estimated based on their relative concentration in vehicle treated mice (steady state concentration) and their production rates p (increase of concentration per time as determined between 0.5 and 2 h after substance treatment) according to:

$t_{½}$ = steady state concentration * ln2/p (Eq. 5)

Immunocytochemistry- Formaldehyde fixed brain halves were embedded into paraffin and sagittally cut into 4 µm sections at three different anatomical levels. Sections were processed as described (Sturchler-Pierrat et al., 1997) and immuno-histochemically stained with antibodies. Aβ specific antibodies were rabbit serum NT11 for total Aβ and end specific mouse monoclonal antibodies 25H10 for Aβ40 and 29C12 for Aβ42 (a gift of P. Paganetti). APP was stained with rabbit sera APP474 raised against purified secreted APP from rat cells or with APP-C8. Glial fibrillary acidic protein (GFAP) as a marker of astrocytes was detected with a rabbit antiserum (Dako M0761, Dako, Glostrup, Denmark). The microglia cells were stained with rabbit antiserum Iba1 obtained from Wako Chemicals (Cat 019741). Bound antibody was visualized by using the avidin-biotin-peroxidase technique (ABC-Elite Kit PK6100; Vector Laboratories, Burlingame, CA). Finally, sections were reacted with diaminobenzidine (DAB) metal enhanced substrate (# 1718096, Roche, Penzberg, Germany) and counterstained with hemalum.

Amyloid plaque load quantification- Amyloid plaque load as % of total area and plaque numbers were measured in neocortex and caudate putamen of NT11 stained sections at three different anatomical levels using a microcomputer assisted imaging software (MCID, version M7 elite, InterFocus Imaging Ltd, Cambridge, England). Microscopic images were digitized by use of a Roper black and white CCD TV camera and stored with 1124x1124 pixel resolution at 256 gray levels. Diffuse amyloid was captured with a detail enhancing function of the software. The pixel size was calibrated using an object micrometer at 5x magnification (Leica Neoplan Objective). Using a motor driven microscope stage for exact positioning of adjacent object fields the entire brain region was analyzed. For each object field the anatomical area

was defined by manual outline. Isolated tissue artifacts were excluded by manual outline.

Statistical analyses- For analysis of APP and its C-terminal fragments, of soluble Aβ and of total Aβ in pre-plaque mice, Student's t-tests (usually 1-tailed) or analysis of variance (ANOVA) followed by post hoc analysis were done (Tukey's test for pairwise comparison of all groups or 1-tailed Dunnett's test for comparison of all treated groups to vehicle). To compare magnitudes of the substance effect on different Aβ species or between different extractions, ANOVA and 1-tailed Dunnett's test were performed on the decadic logarithm of the ratio of the two values. As amyloid loads in plaque bearing mice do not usually show a normal distribution, we used non-parametric tests for these data (Mann-Whitney U-test or the Kruskal-Wallis test followed by post-hoc Tukey's test on ranks; $p<0.05$ considered significant for all tests, analyses done with Systat for Windows 11, Systat Software Inc., San Jose, CA).

Results

The compound used in this study, LY-411575 has previously been described (May et al., 2001; Wong et al., 2004). To determine optimal inhibition, pre-plaque APP23 mice expressing human APP with the KM670/671NL "Swedish" mutation received oral doses between 1 and 10 mg/kg of LY-411575 (supplementary data, Figure 1S). The highest dose of 10 mg/kg was slightly more effective than 3 mg/kg and was chosen for further acute studies.

Kinetics of Aβ and CTFs in pre-plaque APP23 mice after a single γ-secretase inhibitor dose. To analyze the kinetics of Aβ removal *in vivo*, pre-plaque APP23 mice received a single oral dose of 10 mg/kg LY-411575. Following sacrifice at different times thereafter, total Aβ concentrations in forebrains were determined after formic acid extraction whereas CSF and plasma Aβ were analyzed directly. Reduced Aβ40 concentrations were observed in all three compartments as early as 30 min following treatment (Figure 1, A). Thereafter, Aβ40 continued to decrease reaching a minimum at 4-8 h. CSF and plasma Aβ40 decreased faster and to a lower minimum than total Aβ40 in forebrain. Even at 24 h the Aβ40 concentrations in forebrain (-57%, $p<0.001$) and CSF (-48%, $p<0.01$) remained below vehicle values. Of note in plasma Aβ40 recovered more rapidly. At 8 h its concentration was only 18% below vehicle,

compared to at least 80% for CSF and forebrain Aβ40. Thereafter no difference from vehicle treated animals was detectable in plasma. Total Aβ42 in forebrain was less reduced than Aβ40 at all time points up to 24 h (significant between 2 h ($p=0.01$) and 8 h ($p<0.001$ Figure 1, B). However, 53 h after treatment a significant (-19%, $p<0.01$) reduction persisted, while Aβ40 was back to vehicle concentrations. The kinetic difference between the Aβ peptides was confirmed in a separate experiment, where Aβ was analyzed by Western blotting (data not shown). In another study the substance was applied intravenously (1 mg/kg), which did not further accelerate the reduction of Aβ in forebrain (data not shown).

The effect of γ-secretase inhibition on APP C-terminal fragments was analyzed on Western blots of forebrain homogenates (Figure 1, C). For C99 a gradual increase was apparent already at 30 min but leveled off rapidly to reach a maximum at 8 h. After 24 h C99 was still elevated while it had declined to vehicle values at 53 h. In contrast, C83 showed a lag phase followed by a longer increase reaching a maximum at 8-24 h. This demonstrates inhibition of γ-secretase at least until 8 h. Even at 53 h C83 remained considerably above vehicle levels. Overall, the relative increase of C83 was larger than that of C99.

Similar reduction of Aβ following γ-secretase inhibition in APP24 and APP51/16 mice. To test for potential differences between transgenic lines, we analyzed APP24 mice containing the "London" mutation (V717I) in the γ-secretase cleavage region of APP (in addition to the KM670/671NL mutation). Compared to APP23 these mice show the expected increased Aβ42/40 ratio but generate less APP and total Aβ. Forebrain and CSF Aβ were measured at 1 h and 6 h after a 10 mg/kg LY-411575 treatment of pre-plaque APP24 mice (Figure 2, A). Total Aβ40 and Aβ42 were significantly reduced already after 1 h. At both time points, the relative decrease of each of the Aβ species was very similar to the one in APP23 mice (Figure 1, A). The smaller reduction of Aβ42 compared to Aβ40 found in APP23 was confirmed ($p<0.05$ at 6 h). Average Aβ42 in CSF (1.0±0.1 pmol/ml) was reduced by 33% ($p<0.05$) at 1 h and 89% ($p<0.001$) at 6 h, which is a stronger reduction than in forebrain, similar to the observation made for Aβ40 in APP23.

JPET Fast Forward. Published on August 7, 2008 as DOI: 10.1124/jpet.108.140327
This article has not been copyedited and formatted. The final version may differ from this version.

We also studied mice expressing human wild-type APP (pre-plaque APP51/16) treated with 10 mg/kg LY-411575 and sacrificed 6 h later (Figure 2, A). Forebrain showed a 66% decrease in Aβ40 following formic acid extraction, very similar to APP24. For Aβ42 a reduction was also found but could not be quantified reliably. In plasma, Aβ1-40 was reduced by 89% ($p<0.01$). These data demonstrate that the three different APP transgenic mouse lines carrying different mutations respond with similar Aβ reductions to the acute inhibition of γ-secretase.

Differential extraction of a brain Aβ subpopulation undergoing rapid turnover. The maximal reduction of total Aβ40 or Aβ42 achieved after γ-secretase inhibition was lower in brain than in CSF. Considering that CSF Aβ originates from brain, this observation hints to brain Aβ species, which undergo a slower turnover resulting in an incomplete removal. We tried to enrich a subpopulation of Aβ, which is completely removed upon acute γ-secretase inhibition. Forebrains of APP23 mice from the kinetic study were extracted either with formic acid, 1% Triton X-100 or TBS and Aβ40 was quantified (Figure 1, A). In vehicle treated mice, Triton X-100 extracted ~30% and TBS extracted ~2% of total, formic acid soluble Aβ40. The relative reduction of Aβ40 was stronger in the Triton X-100 extract than in the formic acid extract at all time points of the descending part of the kinetics ($p=0.05$ at 4 h and $p=0.016$ at 6 h). The kinetics of Aβ40 in Triton X-100 extracts closely reflected those of CSF. In the TBS extracts the reduction of Aβ40 was even higher than in Triton X-100 extracts, however, the variation was larger (Figure 1, A). Confirming these observations LY-411575-treated APP24 and APP51 mice also showed a stronger Aβ40 reduction in the Triton X-100 compared to the formic acid extract (Figure 2, A).

APP24 mice were used to test for an enrichment of an Aβ42 population with a more rapid turnover. Triton X-100 soluble forebrain Aβ42 was more reduced after LY-411575 treatment than total, formic acid extracted Aβ42 (Figure 2, A; $p<0.05$ at 1 h) and paralleled Aβ42 in CSF better, similar to Aβ40 in APP23. A larger Aβ42 reduction in the Triton X-100 extract (-33% at 1 h, below limit of quantification at 6 h) compared to the formic acid extract (Figure 1, B) was also observed for APP23 mice. These results indicate that subpopulations of Aβ40 and Aβ42 exist in brain of pre-plaque APP transgenic mice, which

differ in stability. They also confirm the similarity of the Aβ reduction in the different transgenic mouse models following γ-secretase inhibition.

Estimation of Aβ half-life and production rate. The decrease of Aβ after γ-secretase blockade allowed us to estimate its half-life by fitting data from the initial inhibition period (Figure 2, B and 3, A) using a first-order model for Aβ reduction (see Methods, Eq. 1). This approach assumes immediate and complete block of Aβ generation, in agreement with brain substance levels being several orders of magnitude above cellular IC_{50} values (see Methods). The calculated values are upper limits of the half-life, however, the good fit indicates that γ-secretase inhibition was obtained rapidly. For APP23 mice the half-life of formic acid extracted, total Aβ40 in forebrain was determined as 1.1 h. This predicts an almost complete disappearance after 4 h, which was not observed, likely reflecting the presence of Aβ subpopulations with considerably longer half-lives. Triton X-100 soluble Aβ40 disappeared with a half-life of 0.7 h and obviously reflects a population with a more rapid turnover. The same value was obtained for CSF Aβ40. Its almost complete loss after 4 h suggests the presence of only one Aβ40 population likely reflecting the soluble and removable fraction of brain Aβ40. The Aβ40 half-life in plasma was calculated as 0.5 h based on a simple first order decline (Figure 3, A), but may be shorter assuming an initial lag phase suggested by the 30 min time point.

For formic acid extracted brain Aβ40 from APP24 mice, a shorter half-life (1.3 h) was calculated than for Aβ42 (2 h) (Figure 2, B). The amount of Aβ42 left after 6 h (50%) was far more than predicted from this half-life (12.5%) concurring with the presence of more stable Aβ42 species as well. However, Aβ42 in Triton X-100 brain extracts showed a faster turn-over ($t_{1/2}$ = 1.7 h) with the same half-life as Aβ42 in CSF. As the brain concentration of Aβ remains about constant in pre-plaque APP transgenic mice, a steady-state between generation and removal of Aβ can be assumed. This allows to estimate the approximate Aβ production rate in forebrain of APP23 mice as 9.3 pmol/g/h for Aβ40 and 0.7 pmol/g/h for Aβ42 (see Methods, Eq. 3). To test the plausibility of these values, we made the simplifying assumption that newly generated Aβ is quantitatively deposited during the phase of exponential plaque growth. We measured

JPET Fast Forward. Published on August 7, 2008 as DOI: 10.1124/jpet.108.140327
This article has not been copyedited and formatted. The final version may differ from this version.

average forebrain Aβ in female APP23 mice at 11 and 18.3 months as 5447 and 65653 pmol/g (Aβ1-40) and as 1668 and 9820 pmol/g (Aβ1-42), respectively. The increase of Aβ concentrations over time allows to roughly estimate the production rates of Aβ40 and 42 in APP23 forebrain as k' = 11 pmol/g/h and 1.5 pmol/g/h, respectively (Methods, Eq. 4). These values are in good agreement with production rates calculated from the Aβ removal kinetics. Overall, these estimations indicate a half-life for soluble, non-deposited Aβ40 and 42 of about 0.7 and 1.7 hours or even less. Additional species exist in brain (e.g. Aβ bound to proteins or molecules in an oligomeric state) with a much longer half-life, which remains to be determined.

The kinetics of APP carboxy-terminal fragments after blockade of γ-secretase were also used to estimate their degradation by this enzyme. We first determined the production rates for both C83 and C99 from the increase between 0.5 and 2 h, This interval accounts for a possible initial lag phase (Figure 3, B). As described in Methods (Eq. 5), the half-lives of C99 and C83 for degradation by γ-secretase were then calculated as about 0.4 and 0.1 h, respectively.

Subchronic inhibition of γ-secretase in pre-plaque APP23 mice. To study the effects of longer γ-secretase inhibition, pre-plaque male APP23 mice were treated for two weeks once daily with 10 mg/kg LY-411575 without signs of overt toxicity. A second set of animals received only a single dose. Mice were sacrificed 6 h or 24 h after the last substance application. Brain Aβ levels were significantly more reduced after the 14 day than after a single treatment at the 6 hr sacrifice point (supplementary data, Figure 2S). This additive effect is consistent with the observation that a single inhibitor dose reduced Aβ for longer than the treatment interval of 24 h (Figure 1). Six and 24 h after the last of 14 substance applications, forebrain Aβ40 was decreased by 94% and 55%, while the Aβ42 reduction reached 89% and 32%, respectively. CTFs accumulated differentially. While the C99 increase in the forebrain was only slightly higher than after a single treatment, the C89/C83-band was considerably stronger after the 14 day treatment (Figure 4, A). Dephosphorylation allowed to identify C83 as the main polypeptide in this band. (Figure 4, C). These data indicate that γ-secretase was still efficiently inhibited after subchronic LY-

JPET Fast Forward. Published on August 7, 2008 as DOI: 10.1124/jpet.108.140327
This article has not been copyedited and formatted. The final version may differ from this version.

411575 treatment.

Chronic inhibition of γ-secretase in APP23 mice during the early phase of amyloid plaque formation. Using a preventive paradigm we next tested if chronic reduction of Aβ production also reduced amyloid plaque formation. Female APP23 mice (20 per group) were treated for 3 months with LY-411575 and sacrificed at 6 h and 24 h after the last treatment. Treatment was started at an age of six months, when plaque formation just begins. Mice received 10 mg/kg/d of drug for 7 days and 3 mg/kg thereafter to improve tolerability because after the first week two (10%) substance treated animals showed weight reduction, sickness behavior and were lost. The side effects were not further analyzed but may have been related to intestinal goblet cell hyperplasia (Wong et al., 2004; Hyde et al., 2006). The body weight of the remaining animals was not reduced during chronic treatment and developed similarly to the non-treated controls. Yet, after about 14 days grey patches started to appear in the normally black coat of substance treated animals (supplementary data, Figure 3S, C) and thymus atrophy was found at sacrifice (data not shown) as previously described (Wong et al., 2004; Hyde et al., 2006). The average forebrain weight of the treated animals was slightly reduced by about 5% ($p<0.05$) and a 2.7 times larger volume of CSF could be collected from these animals ($p<0.001$, supplementary data, Figure 3S, B).

Analysis of total Aβ from forebrains showed that all isoforms measured (Aβ1-38, 40 and 42) were reduced by about 80% following LY-411575 treatment (Figure 5). Data from the subgroups sacrificed 6 and 24 h after the last treatment were pooled as they did not differ significantly. Nonetheless, a trend for higher total Aβ values at the 24 h time point indicated an additional, small contribution of the acute reduction of newly synthesized Aβ. As after the shorter treatments, accumulated C-terminal APP fragments were found (Figure 4). The strongest accumulation was found for C83 while C89 remained a minor portion of the accumulated CTFs (Figure 4, C). Very similar to acute LY-411575 treatment, Aβ1-38, Aβ1-40 and 1-42 concentrations in CSF were reduced by about 85%, 78% and 61%, respectively, 6 h after the last substance application (Figure 5, B). A significant reduction of Aβ in CSF by 30% (Aβ1-38), 43% (Aβ1-40) and 52% (Aβ1-42) was still seen at 24 h. In plasma, analyzed 6 h after the last substance

application, all three Aβ species (Aβ1-38, 40 and 42) were reduced by about 80% in LY-411575 treated animals (not shown).

To test for an effect of the treatment on APP expression and its metabolism we quantified total APP (full-length plus sAPP) and sAPPα and sAPPβ. Total APP on Western blots was slightly decreased in substance treated animals (-13%, p=0.008, 2-tailed t-test). Average levels of sAPPα (15±1 µg/g in controls) and sAPPβ (53±5 µg/g in controls) were also significantly reduced (-6%, $p<0.01$ and -18%, $p<0.001$, respectively, 2-tailed t-test). While these changes may indicate a general treatment effect, they are much smaller than the Aβ reductions observed in the different compartments. We also tested for a compensatory upregulation of presenilin during the long-term γ-secretase inhibition and probed forebrain Western blots with antibodies against the presenilin 1 CTF, but did not detect a difference between the LY-411575 and vehicle group (data not shown).

Quantitative immunohistochemistry of the neocortical amyloid load revealed no difference between animals sacrificed at 6 or 24 h after the last treatment, hence both groups were combined for analysis. Compared to the vehicle treated animals, a 80% reduction of the neocortical plaque area was found in the treated group (Figure 6, A-D), which was identical in size to the biochemically determined effect. While the neocortical area covered by plaques exceeded 0.1% in 65% of the vehicle treated animals, all mice receiving LY-411575 had a plaque area below 0.1%. The median cortical plaque number was reduced by 66% from 4.6 to 1.6 plaques per mm^2, i.e. less than the median plaque area in agreement with a stronger effect on Aβ deposition than on de novo plaque formation.

Following 3 months of LY-411575 treatment, a morphological change of intra-neuronal Aβ was observed in cortical pyramidal cells. Whereas the Aβ distribution was mostly homogeneous in control mice, treated animals showed strongly stained clusters (Figure 6, E, F). This change in Aβ distribution was found in cerebral cortex and subiculum, regions forming the first amyloid plaque deposits. It was not observed in the hippocampus proper, where plaque formation starts somewhat later. End-specific Aβ40 and Aβ42 antibodies also reacted with these clusters (supplementary data, Figure 4S) confirming their Aβ content rather than a cross-reaction with APP. Consistent with this notion, staining of neuronal cell bodies for

JPET Fast Forward. Published on August 7, 2008 as DOI: 10.1124/jpet.108.140327
This article has not been copyedited and formatted. The final version may differ from this version.

APP with antibodies recognizing its N- or C-terminus was reduced in LY-411575 treated animals (Figure 7). This included neocortical as well as hippocampal neurons, suggesting a reduction of APP in certain brain regions of treated animals, in accordance with the reduced APP measured biochemically. In contrast, APP C-terminal antibodies strongly stained nerve fibers in several brain regions of LY-411575 treated animals (Figure 7, B, D). This staining most likely reflected accumulated C-terminal fragments of APP rather than full length APP, as these structures were not stained by a N-terminal APP antibody (Figure 7, E, F).

To analyze for an effect on plaque-associated gliosis, we quantified astrocyte (GFAP) and microglia (Iba1) stainings. At the low amyloid plaque load in 9 months old APP23 mice, these markers were not generally increased compared to non-transgenic animals but rather redistributed resulting in an association with plaques. Accordingly, the GFAP and Iba1 labeled surface areas in cerebral cortex or hippocampus remained unchanged by the treatment. However, the Iba1 positive area was increased (+ 31%, p= 0.01, 2-tailed t-test) in the cerebellum of LY-411575 treated mice indicating some microglia activation. This probably is a substance effect unrelated to the plaque reduction, as plaques are not formed in cerebellum of APP23 mice.

Chronic γ-secretase inhibition of plaque bearing mice. As AD patients already contain amyloid deposits in brain at diagnosis we also determined if chronic γ-secretase inhibition would be effective in the presence of preexisting plaques. Furthermore, to reproduce the effect in an independent mouse model we used APP24 mice with a more diffuse, AD-like plaque morphology. A baseline group was sacrificed at 15 months while other animals were treated during 2 months with daily oral doses of 3 mg/kg LY-411575 or vehicle and sacrificed 6 h after the last substance application. None of the mice died during the treatment but animals receiving LY-411575 also showed the coat color changes described above.

In forebrain of the vehicle group, median Aβ1-38, 40 and 42 concentrations were 29, 37 and 57% higher than at baseline reflecting the increase in Aβ deposition during the 2 months treatment period (Figure 8, A). In contrast, in the LY-411575 treated group forebrain Aβ remained at baseline level. The olfactory bulb also showed a significant increase of Aβ peptides in the vehicle group, which was largely inhibited

by substance treatment (not shown). Both forebrain and olfactory bulb already contained a considerable amyloid load at the start of the experiment. To analyze the treatment effect at the onset of plaque formation as in the previous study, Aβ was also determined in pons/medulla oblongata, which contains only very few plaques in 15-17 months old APP24 mice. In this brain region, Aβ1-38 and 1-40 remained at baseline in the vehicle group suggesting that they are not yet deposited (Figure 8, B). Confirming this notion, LY-411575 reduced both peptides below baseline which indicates turnover. In contrast, Aβ1-42 was 3-4 times higher in the vehicle group compared to baseline reflecting the formation of early amyloid deposits. This increase was only partially inhibited in LY-411575 treated animals. In CSF average Aβ42 (0.9±0.2 pmol/ml) was reduced by 77% ($p<0.001$, 2-tailed t-test) compared to vehicle treated animals demonstrating that an acute Aβ reduction in CSF still occurs in plaque bearing mice.

The median plaque area of the 15 months old baseline group was 1.8% in neocortex (Figure 9, D). Two months later, it increased to 5% in vehicle treated animals. LY-411575 significantly lowered the neocortical plaque area to 4% corresponding to a reduction of further amyloid deposition by 31% ($p=0.01$, 2-tailed Mann-Whitney U-test). In caudate putamen, which has a lower amyloid load than neocortex (median plaque area at baseline: 0.16%, vehicle group: 1.6%), LY-411575 had a more pronounced effect (plaque area of 0.5%, corresponding to a 79% reduction of further amyloid deposition, $p=0.001$, 2-tailed Mann-Whitney U-test). Both, plaque area and treatment effect were similar to the corresponding data for neocortex of the 9 months old APP23 mice described above. The effects on plaque number were comparable to those on plaque area (Figure 9, E) indicating no specific effect on Aβ deposition versus de novo plaque formation. As expected, hardly any plaques could be detected in pons/medulla oblongata. No indication for a removal of preexisting plaques during the two months treatment was found in the brain regions examined.

Discussion

In this study we have blocked γ-secretase with a potent inhibitor to analyze Aβ turnover and deposition in different APP transgenic mouse models at several stages of amyloid formation. Acute γ-secretase

inhibition in pre-plaque mice resulted in a dose-dependent decrease of brain Aβ and a corresponding increase in APP CTFs. These effects were more pronounced after subchronic treatment. Mice transgenic for wildtype human APP (APP51/16) responded to the same extent as APP23 carrying the "Swedish" mutation at the BACE cleavage site and APP24, which in addition contain the "London" mutation within the γ-secretase cleavage region.

The inhibitor used, LY-411575, rapidly achieves a high brain concentration (Cirrito et al., 2003; Lanz et al., 2004; methods this study) allowing for kinetic studies. Aβ reached a minimum in brain, CSF and plasma at 4-8 h after substance application and recovered only partially until 24 h indicating a long-lasting inhibitor effect. The turnover of Aβ40 was generally more rapid than of Aβ42. CSF Aβ40 and 42 both declined slightly faster and to a lower level than total, formic acid extracted forebrain Aβ. Their decline in TBS and Triton X-100-soluble brain extracts, however, matched the reduction in CSF well suggesting at least two pools in brain: readily soluble Aβ with a half-life of about 0.7 h (Aβ40) and 1.7 h (Aβ42) as well as a less soluble, more stable pool. For both Aβ species the half-lives in the soluble pool and in CSF were almost identical. It is likely that CSF Aβ directly originates from the soluble brain pool, which at least in part is rapidly transported from the parenchyma to CSF and rapidly removed from there. The origin of Aβ from CNS neurons in these mice (Calhoun et al., 1998) further supports this notion. This first direct comparison of the dynamics of the different Aβ pools in brain and CSF indicates that CSF Aβ40 and Aβ42 are suited markers for the corresponding peptides in the soluble brain pool.

A rapid decline of detergent extracted brain Aβ after γ-secretase inhibition has also been found in rats (Best et al., 2005), guinea pigs (Anderson et al., 2005) and Tg2576 mice (Barten et al., 2005), where an Aβ40 half-life of 0.63 h was determined with another γ-secretase (BMS-299897) in very good agreement with this study. As these calculations all assume immediate and complete inhibition of Aβ generation, the real turnover may be even faster. Aβ half-life determinations in human CSF following γ-secretase inhibition are currently not available (see Siemers et al., 2007). Longer Aβ half-lives have been measured in the brain interstitial fluid of LY-411575 treated PDAPP mice by in vivo microdialysis (~2 h for young

mice (Cirrito et al., 2003)) and in human CSF with an isotopic labeling method (clearance rate ~8% per hour, corresponding half-life ~8-9 h (Bateman et al., 2006)). The different techniques used may have contributed to the discrepancies.

The half-life of plasma Aβ40 (≤ 0.5 h) was shorter than in brain and CSF in line with the faster turnover observed in other APP transgenic mouse models (Wong et al., 2004; Barten et al., 2005; Anderson et al., 2005). In plasma Aβ returned to baseline levels more rapidly than in brain and CSF although the human Aβ measured originates from brain. The APP overexpression in APP23 mice may have overloaded the export system to plasma. Under such conditions a minor recovery of brain Aβ is sufficient to completely restore the plasma Aβ. Conversely, a lag phase is expected at the beginning of the decline. A rebound increase in plasma Aβ after γ-secretase inhibitor treatment has been described for humans (e.g. Siemers et al., 2007), guinea pigs (Lanz et al., 2006) and in one (Prasad et al., 2007) but not other (e.g. Wong et al., 2004; Barten et al., 2005; Anderson et al., 2005) APP transgenic mouse studies. It is not accompanied by a change in brain or CSF Aβ suggesting a peripheral origin (as discussed in Siemers et al., 2007). We have not detected a rebound increase in plasma Aβ, perhaps because human Aβ in APP23 originates almost exclusively from brain (Calhoun et al., 1998) but other possibilities (e.g. rebound between 24 and 53 h) cannot be excluded.

An estimate of the Aβ production rate in APP23 mice was obtained from its rate of removal, which is equal assuming Aβ steady-state in pre-plaque mice. The production rate was independently estimated from the Aβ accumulation in plaque bearing APP23 mice supposing that all produced Aβ is deposited. The values obtained with these entirely different approaches were remarkably similar (Aβ40: 9.3 and 11 pmol/g/h, Aβ42: 0.7 and 1.5 pmol/g/h) but in both cases higher for plaque-bearing mice. It, therefore, seems possible that Aβ generation increases during plaque formation. Moreover, the presence of Aβ in CSF of plaque-bearing mice demonstrates its incomplete deposition and suggests even higher actual production rates.

Together with the Aβ reduction, acute γ-secretase inhibition caused a strong elevation of the APP C-

terminal fragments from which the half-lives of C99 and C83 for degradation by γ-secretase were estimated as about 0.4 and 0.1 h, respectively. The reason for this difference is not understood but may be related to different intracellular locations of both fragments. The Swedish mutation as present in APP23 mice is thought to elevate BACE1 cleavage and C99 generation in secretory compared to endocytic compartments (Haass et al., 1995). Future studies will have to show if the same half-lives are obtained with wild-type APP transgenic mice. The continuous increase of C83 during the phase of γ-secretase inhibition indicated that this enzyme serves as its primary degradation pathway in brain neurons. In contrast, the decrease in C99 accumulation with time suggests that this fragment may undergo degradation by proteases different from γ-secretase or that its generation is reduced by feedback mechanisms. It also remains to be determined whether γ-secretase inhibition of wild-type mice, which express far less APP, leads to similar increases in APP CTFs.

Chronic inhibition of γ-secretase in a preventive setting, where APP23 mice had been treated between 6 and 9 months of age, resulted in an 80% reduction of the amyloid plaque area as well as of all three Aβ peptides analyzed (Aβ1-38, 1-40 and 1-42). The number of plaques was less reduced consistent with a smaller effect on de novo plaque formation than on Aβ deposition. Comparable effects have been obtained in PDAPP mice (May et al., 2001). In a clinically more relevant therapeutic paradigm, plaque bearing APP24 mice were treated from 15 to 17 months of age. Forebrain Aβ levels remained at baseline, while the amyloid load increased, yet about 30% less than in the vehicle group. Caudate/putamen, a region with a low plaque development, showed a much stronger reduction of the amyloid load than forebrain of the same mice indicating that the efficacy differences were not age-related. Instead they inversely correlated with the initial amyloid load (Table 1) irrespective of the brain region and amyloid type. These results demonstrate that inhibition of Aβ generation can effectively slow down further amyloid formation in brains already containing plaques, even when the block of Aβ generation is not complete. The reduction is region-specific insofar as a strong effect can be expected for areas with a low amyloid load while it may be much smaller in amyloid laden regions of the same brain. In agreement with

our data an about 50% reduction of plaques was observed after 3 months treatment of aged Tg2576 mice with the γ-secretase inhibitor MRK-560 (Best et al., 2007). Our studies did not provide evidence for a clearance of preexisting plaques in any brain region. Even chronic suppression of APP expression in transgenic mice during 6 months only halted further amyloid deposition (Jankowsky et al., 2005).

At 15 to 17 months plaque formation just starts in pons/medulla oblongata of APP24 mice. In this region, the last γ-secretase inhibitor treatment acutely reduced Aβ1-38 and Aβ1-40 below baseline and vehicle levels similar to forebrain of pre-plaque animals. In contrast, Aβ1-42 increased in the vehicle group indicating deposition, which was partially reduced by the treatment. This supports the notion that Aβ42 initiates deposition in vivo and suggests some independence between the Aβ isoforms, at least initially. In line with these results, CSF Aβ from aged mice with a high brain amyloid load showed a similar reduction after the last γ-secretase inhibitor dose as in acutely treated pre-plaque mice. CSF Aβ, therefore, seems a suited marker to assess treatment effects on Aβ generation in amyloid bearing brain.

As suggested by the acute studies, chronic γ-secretase inhibition caused dramatic elevation of APP C-terminal fragments. Histological analysis of three months treated mice showed that CTFs accumulated primarily in nerve fibers, rather than in cell bodies. Toxic properties have repeatedly been attributed to these fragments (Lee et al., 2006) and their accumulation may lead to side effects. However, the major contribution to side effects of γ-secretase inhibitors is thought to originate from the interference with intestinal and lymphatic cell differentiation associated with the inhibition of Notch cleavage (Searfoss et al., 2003; Wong et al., 2004). Recently, the coat color changes have also been linked to the inhibition of Notch processing (Schouwey and Beermann, 2008). Interestingly, alterations in hair color have also been observed in a clinical study with γ-secretase inhibitor LY-450139 (E. Siemers at the Alzheimer's Association Prevention Conference 2007; http://www.alz.org/preventionconference/pc2007/releases/-61107_130pm_latebreak.asp).

Independent of the potential liabilities of γ-secretase inhibition, our study describes typical features of Aβ turnover and deposition in vivo, which are important to design studies for testing Aβ lowering

approaches. It demonstrates the suitability of APP transgenic mice as translational models for the evaluation of such strategies.

Acknowledgments

We thank Dr. Paolo Paganetti for antiserum NT11 and antibodies 25H10 and 29C12, and Albert Enz for the determination of LY-411575 compound concentrations.

References

Anderson JJ, Holtz G, Baskin PP, Turner M, Rowe B, Wang B, Kounnas MZ, Lamb BT, Barten D, Felsenstein K, McDonald I, Srinivasan K, Munoz B and Wagner SL (2005) Reductions in beta-amyloid concentrations in vivo by the gamma-secretase inhibitors BMS-289948 and BMS-299897. *Biochem Pharmacol* **69**:689-698.

Barten DM, Guss VL, Corsa JA, Loo A, Hansel SB, Zheng M, Munoz B, Srinivasan K, Wang B, Robertson BJ, Polson CT, Wang J, Roberts SB, Hendrick JP, Anderson JJ, Loy JK, Denton R, Verdoorn TA, Smith DW and Felsenstein KM (2005) Dynamics of β-Amyloid Reductions in Brain, Cerebrospinal Fluid, and Plasma of β-Amyloid Precursor Protein Transgenic Mice Treated with a γ-Secretase Inhibitor. *J Pharmacol Exp Ther* **312**:635-643.

Bateman RJ, Munsell LY, Morris JC, Swarm R, Yarasheski KE and Holtzman DM (2006) Human amyloid-beta synthesis and clearance rates as measured in cerebrospinal fluid in vivo. *Nat Med* **12**:856-861.

Baumann K, Paganetti PA, Sturchler-Pierrat C, Wong C, Hartmann H, Cescato R, Frey P, Yankner BA, Sommer B and Staufenbiel M (1997) Distinct processing of endogenous and overexpressed recombinant presenilin 1. *Neurobiol Aging* **18**:181-189.

Best JD, Jay MT, Otu F, Ma J, Nadin A, Ellis S, Lewis HD, Pattison C, Reilly M, Harrison T, Shearman MS, Williamson TL and Atack JR (2005) Quantitative measurement of changes in amyloid-beta(40) in the rat brain and cerebrospinal fluid following treatment with the gamma-secretase inhibitor LY-411575 [N2-[(2S)-2-(3,5-difluorophenyl)-2-hydroxyethanoyl]-N1-[(7S)-5-methyl-6-ox o-6,7-dihydro-5H-dibenzo[b,d]azepin-7-yl]-L-alaninamide]. *J Pharmacol Exp Ther* **313**:902-908.

Best JD, Smith DW, Reilly MA, O'donnell R, Lewis HD, Ellis S, Wilkie N, Rosahl TW, Laroque P, Boussiquet-Leroux C, Churcher I, Atack JR, Harrison T and Shearman MS (2007) The novel γ-secretase inhibitor MRK-560 reduces amyloid plaque deposition without evidence of Notch-related pathology in the Tg2576 mouse. *J Pharmacol Exp Ther* **320**:552-558.

Calhoun ME, Wiederhold KH, Abramowski D, Phinney AL, Probst A, Sturchler-Pierrat C, Staufenbiel M, Sommer B and Jucker M (1998) Neuron loss in APP transgenic mice. *Nature* **395**:755-756.

Churcher I, Beher D, Best JD, Castro JL, Clarke EE, Gentry A, Harrison T, Hitzel L, Kay E, Kerrad S, Lewis HD, Morentin-Gutierrez P, Mortishire-Smith R, Oakley PJ, Reilly M, Shaw DE, Shearman MS, Teall MR, Williams S and Wrigley JD (2006) 4-substituted cyclohexyl sulfones as potent, orally active gamma-secretase inhibitors. *Bioorg Med Chem Lett* **16**:280-284.

Cirrito JR, May PC, O'Dell MA, Taylor JW, Parsadanian M, Cramer JW, Audia JE, Nissen JS, Bales KR, Paul SM, DeMattos RB and Holtzman DM (2003) In vivo assessment of brain interstitial fluid with microdialysis reveals plaque-associated changes in amyloid-beta metabolism and half-life. *J Neurosci* **23**:8844-8853.

Citron M, Westaway D, Xia W, Carlson G, Diehl T, Levesque G, Johnson-Wood K, Lee M, Seubert P, Davis A, Kholodenko D, Motter R, Sherrington R, Perry B, Yao H, Strome R, Lieberburg I, Rommens J, Kim S, Schenk D, Fraser P, St George HP and Selkoe DJ (1997) Mutant presenilins of Alzheimer's disease increase production of 42-residue amyloid beta-protein in both transfected cells and transgenic mice. *Nat Med* **3**:67-72.

Comery TA, Martone RL, Aschmies S, Atchison KP, Diamantidis G, Gong X, Zhou H, Kreft AF, Pangalos MN, Sonnenberg-Reines J, Jacobsen JS and Marquis KL (2005) Acute gamma-secretase inhibition improves contextual fear conditioning in the Tg2576 mouse model of Alzheimer's disease. *J Neurosci* **25**:8898-8902.

Dash PK, Moore AN and Orsi SA (2005) Blockade of gamma-secretase activity within the hippocampus enhances long-term memory. *Biochem Biophys Res Commun* **338**:777-782.

Donoviel DB, Hadjantonakis AK, Ikeda M, Zheng H, Hyslop PS and Bernstein A (1999) Mice lacking both presenilin genes exhibit early embryonic patterning defects. *Genes Dev* **13**:2801-2810.

Dovey HF, John V, Anderson JP, Chen LZ, de Saint AP, Fang LY, Freedman SB, Folmer B, Goldbach E, Holsztynska EJ, Hu KL, Johnson-Wood KL, Kennedy SL, Kholodenko D, Knops JE, Latimer LH, Lee M, Liao Z, Lieberburg IM, Motter RN, Mutter LC, Nietz J, Quinn KP, Sacchi KL, Seubert PA, Shopp

GM, Thorsett ED, Tung JS, Wu J, Yang S, Yin CT, Schenk DB, May PC, Altstiel LD, Bender MH, Boggs LN, Britton TC, Clemens JC, Czilli DL, Dieckman-McGinty DK, Droste JJ, Fuson KS, Gitter BD, Hyslop PA, Johnstone EM, Li WY, Little SP, Mabry TE, Miller FD and Audia JE (2001) Functional gamma-secretase inhibitors reduce beta-amyloid peptide levels in brain. *J Neurochem* **76**:173-181.

Haass C, Lemere CA, Capell A, Citron M, Seubert P, Schenk D, Lannfelt L, Selkoe DJ (1995) The Swedish mutation causes early-onset Alzheimer's disease by beta-secretase cleavage within the secretory pathway. *Nat Med*. **1**:1291-1296.

Hardy J and Selkoe DJ (2002) The amyloid hypothesis of Alzheimer's disease: progress and problems on the road to therapeutics. *Science* **297**:353-356.

Herzig MC, Winkler DT, Burgermeister P, Pfeifer M, Kohler E, Schmidt SD, Danner S, Abramowski D, Sturchler-Pierrat C, Burki K, van Duinen SG, Maat-Schieman ML, Staufenbiel M, Mathews PM and Jucker M (2004) Abeta is targeted to the vasculature in a mouse model of hereditary cerebral hemorrhage with amyloidosis. *Nat Neurosci* **7**:954-960.

Hyde LA, McHugh NA, Chen J, Zhang Q, Manfra D, Nomeir AA, Josien H, Bara T, Clader JW, Zhang L, Parker EM and Higgins GA (2006) Studies to investigate the in-vivo therapeutic window of the γ-secretase inhibitor LY411,575 in the CRND8 mouse. *J Pharmacol Exp Ther* **319**:1133-1143.

Jankowsky JL, Slunt HH, Gonzales V, Savonenko AV, Wen JC, Jenkins NA, Copeland NG, Younkin LH, Lester HA, Younkin SG and Borchelt DR (2005) Persistent Amyloidosis following Suppression of Abeta Production in a Transgenic Model of Alzheimer Disease. *PLoS Med* **2**:e355.

Klafki HW, Wiltfang J and Staufenbiel M (1996) Electrophoretic separation of betaA4 peptides (1-40) and (1-42). *Anal Biochem* **237**:24-29.

Lanz TA, Hosley JD, Adams WJ and Merchant KM (2004) Studies of Abeta pharmacodynamics in the brain, cerebrospinal fluid, and plasma in young (plaque-free) Tg2576 mice using the gamma-secretase inhibitor N2-[(2S)-2-(3,5-difluorophenyl)-2-hydroxyethanoyl]-N1-[(7S)-5-methyl-6-oxo -6,7-dihydro-5H-dibenzo[b,d]azepin-7-yl]-L-alaninamide (LY-411575). *J Pharmacol Exp Ther* **309**:49-55.

Lanz TA, Karmilowicz MJ, Wood KM, Pozdnyakov N, Du P, Piotrowski MA, Brown TM, Nolan CE, Richter KE, Finley JE, Fei Q, Ebbinghaus CF, Chen YL, Spracklin DK, Tate B, Geoghegan KF, Lau LF, Auperin DD and Schachter JB (2006) Concentration-dependent modulation of Aβ in vivo and in vitro using the γ-secretase inhibitor, LY- 450139. *J Pharmacol Exp Ther* **319**:924-933.

Lee KW, Im JY, Song JS, Lee SH, Lee HJ, Ha HY, Koh JY, Gwag BJ, Yang SD, Paik SG and Han PL (2006) Progressive neuronal loss and behavioral impairments of transgenic C57BL/6 inbred mice expressing the carboxy terminus of amyloid precursor protein. *Neurobiol Dis* **22**:10-24.

Li J, Fici GJ, Mao CA, Myers RL, Shuang R, Donoho GP, Pauley AM, Himes CS, Qin W, Kola I, Merchant KM and Nye JS (2003) Positive and negative regulation of the gamma-secretase activity by nicastrin in a murine model. *J Biol Chem* **278**:33445-33449.

May PC, Altstiel LD, Bender MH, Boggs LN, Calligaro DO, Fuson KS, Gitter BD, Hyslop PA, Jordan WH, Li WY, Mabry TE, Mark RJ, Ni B, Nissen JS, Porter WJ, Sorgen SG, Su Y, Audia JE, Dovey HF, Games D, John V, Freedman S, Guido T, Johnson-Wood KL, Khan K, Latimer LH, Lieberburg IM, Seubert PA, Soriano F, Thorsett ED and Schenk DB (2001) Marked reduction of Abeta accumulation and beta-amyloid plaque pathology in mice upon chronic treatment with a functional gamma-secretase inhibitor. *Soc Neurosci Abstr* **27**:681

Prasad CV, Zheng M, Vig S, Bergstrom C, Smith DW, Gao Q, Yeola S, Polson CT, Corsa JA, Guss VL, Loo A, Wang J, Sleczka BG, Dangler C, Robertson BJ, Hendrick JP, Roberts SB and Barten DM (2007) Discovery of (S)-2-((S)-2-(3,5-difluorophenyl)-2-hydroxyacetamido)-N-((S,Z)-3-methyl-4- oxo-4,5-dihydro-3H-benzo[d][1,2]diazepin-5-yl)propanamide (BMS-433796): A gamma-secretase inhibitor with Abeta lowering activity in a transgenic mouse model of Alzheimer's disease. *Bioorg Med Chem Lett* **17**:4006-4011.

Saura CA, Chen G, Malkani S, Choi SY, Takahashi RH, Zhang D, Gouras GK, Kirkwood A, Morris RG and Shen J (2005) Conditional inactivation of presenilin 1 prevents amyloid accumulation and temporarily rescues contextual and spatial working memory impairments in amyloid precursor protein transgenic mice. *J Neurosci* **25**:6755-6764.

Scheuner D, Eckman C, Jensen M, Song X, Citron M, Suzuki N, Bird TD, Hardy J, Hutton M, Kukull W, Larson E, Levy-Lahad E, Viitanen M, Peskind E, Poorkaj P, Schellenberg G, Tanzi R, Wasco W, Lannfelt L, Selkoe D and Younkin S (1996) Secreted amyloid beta-protein similar to that in the senile plaques of Alzheimer's disease is increased in vivo by the presenilin 1 and 2 and APP mutations linked to familial Alzheimer's disease. *Nat Med* **2**:864-870.

Schouwey K and Beermann F (2008) The Notch pathway: hair graying and pigment cell homeostasis. *Histol Histopathol* **23**:609-619.

Schrader-Fischer G and Paganetti PA (1996) Effect of alkalizing agents on the processing of the beta-amyloid precursor protein. *Brain Res* **716**:91-100.

Searfoss GH, Jordan WH, Calligaro DO, Galbreath EJ, Schirtzinger LM, Berridge BR, Gao H, Higgins MA, May PC and Ryan TP (2003) Adipsin, a biomarker of gastrointestinal toxicity mediated by a functional gamma-secretase inhibitor. *J Biol Chem* **278**:46107-46116.

Selkoe D and Kopan R (2003) Notch and Presenilin: regulated intramembrane proteolysis links development and degeneration. *Annu Rev Neurosci* **26**:565-597.

Shearman MS, Beher D, Clarke EE, Lewis HD, Harrison T, Hunt P, Nadin A, Smith AL, Stevenson G and Castro JL (2000) L-685,458, an aspartyl protease transition state mimic, is a potent inhibitor of amyloid beta-protein precursor gamma-secretase activity. *Biochemistry* **39**:8698-8704.

Siemers ER, Dean RA, Friedrich S, Ferguson-Sells L, Gonzales C, Farlow MR and May PC (2007) Safety, Tolerability, and Effects on Plasma and Cerebrospinal Fluid Amyloid-beta After Inhibition of gamma-Secretase. *Clin Neuropharmacol* **30**:317-325.

Sturchler-Pierrat C, Abramowski D, Duke M, Wiederhold KH, Mistl C, Rothacher S, Ledermann B, Burki K, Frey P, Paganetti PA, Waridel C, Calhoun ME, Jucker M, Probst A, Staufenbiel M and Sommer B (1997) Two amyloid precursor protein transgenic mouse models with Alzheimer disease-like pathology. *Proc Natl Acad Sci U S A* **94**:13287-13292.

Tandon A and Fraser P (2002) The presenilins. *Genome Biol* **3**:3014.

Wolfe MS (2006) The gamma-secretase complex: membrane-embedded proteolytic ensemble. *Biochemistry* **45**:7931-7939.

Wong GT, Manfra D, Poulet FM, Zhang Q, Josien H, Bara T, Engstrom L, Pinzon-Ortiz M, Fine JS, Lee HJ, Zhang L, Higgins GA and Parker EM (2004) Chronic treatment with the gamma-secretase inhibitor LY-411,575 inhibits beta-amyloid peptide production and alters lymphopoiesis and intestinal cell differentiation. *J Biol Chem* **279**:12876-12882.

Wong PC, Zheng H, Chen H, Becher MW, Sirinathsinghji DJ, Trumbauer ME, Chen HY, Price DL, Van der Ploeg LH and Sisodia SS (1997) Presenilin 1 is required for Notch1 and DII1 expression in the paraxial mesoderm. *Nature* **387**:288-292.

Zhao G, Cui MZ, Mao G, Dong Y, Tan J, Sun L and Xu X (2005) gamma-Cleavage is dependent on zeta-cleavage during the proteolytic processing of amyloid precursor protein within its transmembrane domain. *J Biol Chem* **280**:37689-37697.

Legends for Figures

Figure 1 Kinetics of Aβ reduction and CTF accumulation in pre-plaque APP23 mice after application of LY-411575.

Male APP23 mice (hAPP, Swedish mutation, 6-8 per group) were treated with 10 mg/kg LY-411575 or vehicle at 4 months of age and sacrificed at 0.5, 1, 2, 4, 6, 8, 24 or 53 h. Aβ in forebrain and CSF was determined by ELISA while an electrochemoluminescence-linked immunoassay was used for plasma; C99 and C83 were measured by Western blotting (antiserum APP-C8). A: Time-dependent reduction of total (formic acid extracted), Triton X-100 soluble and TBS-soluble Aβ40 in forebrain and total Aβ40 in CSF and plasma. B: Comparison of total Aβ40 and Aβ42 reductions in forebrain. C: Accumulation of C99 and C83 in forebrain. Significant differences to the vehicle group are indicated by asterisks (ANOVA and Dunnett's test; $p<0.05$: *; $p<0.01$: **; $p<0.001$: ***). In forebrain of vehicle treated animals, total Aβ40 and Aβ42 concentrations were 21±0.3 pmol/g and 6±0.3 pmol/g (average±standard error). Triton X-100 and TBS solubilized about 30% and 2% of total Aβ40. In CSF and plasma Aβ40 was at 17% and 0.4% of the forebrain level, respectively.

Figure 2 Reduction of Aβ in pre-plaque APP24 and APP51/16 mice after LY-411575 treatment.

Female APP24 mice (hAPP, Swedish and London mutations) at 4 months of age and male APP51/16 mice (hAPP, wild-type) at 6 months received a single dose of LY-411575 (10 mg/kg) or vehicle and were sacrificed 1 h (APP24 only) and 6 h thereafter (5-6 per group). Following extraction of forebrain homogenates with formic acid (FA, total) or 1% Triton X-100 (Tx100), Aβ concentrations in forebrain were determined by ELISA (FA) or electrochemiluminescence-linked immunoassay (Tx100). A: In APP24 forebrain, Aβ40 and Aβ42 were significantly reduced in a time-dependent manner. The reduction was more pronounced for Aβ40 than for Aβ42 and stronger for Triton X-100 soluble than for total Aβ. The Aβ40 reduction in APP51/16 mice was similar to APP24. B: The fitted curves of Aβ decrease in APP24 mice were used to calculate half-lives ($t_{1/2}$) and rate constants for the reduction (k) of total (FA)

and Triton X-100 (Tx100) soluble forebrain and CSF Aβ. The Aβ42 reduction in CSF was very similar to Triton extracts of forebrain. Significant differences between treatment groups and vehicle are indicated by asterisks (ANOVA and Dunnett's test for APP24, t-test for APP51/16; $p<0.05$: *; $p<0.01$: **; $p<0.001$: ***; n.d.: below detection limit). In forebrain of vehicle treated APP24 animals, total Aβ40 and Aβ42 concentrations were 6.7±0.5 pmol/g and 6.3±0.7 pmol/g (average±standard error). Triton X-100 solubilized about 58% of total Aβ40 and 22% of total Aβ42. In CSF Aβ42 was at 16% of the forebrain level. In forebrain of vehicle treated APP51/16 mice, the total Aβ40 concentration was 7±0.6 pmol/g.

Figure 3 Aβ and CTF halflives in pre-plaque APP23 mice.

Data from Figure 1 were used: A: Decrease of Aβ during the first 4 h after substance application. The fitted curves were used to calculate half-lives ($t_{1/2}$) and rate constants for the reduction (k) of total (FA) and Triton X-100 (Tx100) soluble Aβ40 in forebrain, CSF and plasma. Please note that the plasma data did not follow a first order decline from 0 h on. The brain Aβ42 half-life could not be determined reliably during the 4 h period. B: While accumulation of C99 was highest between 0.5 and 1 h after substance treatment and leveled off thereafter, C83 accumulated linearly between 0.5 and 8 h (Pearson correlation coefficient $p=0.96$). Halflives of C99 (0.4 h) and C83 (0.1 h) were calculated from accumulation in the highlighted time interval (0.5 – 2 h after LY-411575 treatment).

Figure 4 C-terminal APP-fragments after acute, subchronic and chronic treatment of APP23 mice with LY-411575.

Animals received a single, 14 d or 3 months treatment with LY-411575. A: Western blot of representative animals demonstrating that APP C-terminal fragments were increased compared to controls (no) already after a single dose and raised further upon prolonged treatment (14 days and 3 months). After chronic treatment (3 mo), new bands were detected (see bracket with asterisk), which may represent APP degradation products or aggregated CTFs. Animals sacrificed 6 h after substance treatment are shown. B: Even after chronic treatment with LY-411575 (3 months), the increase of C99 in forebrain partially normalized towards control values 24 h after the last treatment (ANOVA and Tukey's test; $p<0.01$: **;

p<0.001: ***). C: Dephosphorylation with E.coli λ-phosphatase revealed that the main accumulating CTF of APP was C83. C89 also accumulated slightly more than C99 (compare second to last lane). Western blots were done with antiserum APP-C8.

Figure 5 Chronic LY-411575 treatment of APP23 mice during the early stage of plaque formation reduced forebrain and CSF Aβ.

Female APP23 mice (20 per group) were treated for 3 months with LY-411575 starting at an age of 6 months and sacrificed at 6 h and 24 h after the last treatment. Aβ was analyzed by Western blotting. A: Median Aβ1-38, 40 and 42 concentrations in forebrain were reduced by 81%, 85% and 77% compared to control animals. Data from both sacrifice points were combined. B: Aβ species in CSF were decreased compared to vehicle 6 h after drug application and normalized partially towards control values 24 h after the treatment. Each symbol represents one animal. The lines shows the position of medians (forebrain) or average (CSF), respectively (determined by Western blotting with antibody 6E10, forebrain: Mann-Whitney U-test; p<0.0001: ***; CSF: ANOVA and Dunnett's test; p<0.05: *; p<0.01: **; p<0.001: ***).

Figure 6 Chronic LY-411575 treatment during the early stage of plaque formation reduced amyloid plaque deposition.

At 9 months, amyloid plaques in APP23 brains are mainly restricted to the neocortex, medium in size (10-50 µm diameter) and mostly of the compact type. A: After treatment from 6 to 9 months, the plaque area in neocortex was reduced by 80%. B: The number of plaques per mm^2 decreased by 66% (Mann-Whitney U-test: p<0.0001). Each symbol represents one animal. The lines indicate the median. C, D: Representative forebrain sections stained for amyloid plaques (arrowheads) using antibody NT11. E, F: Intracellular Aβ in cortical pyramidal cells of substance treated animals formed clusters strongly stained with the Aβ antiserum NT11 (arrows in F) and with antibodies specific for Aβ40 and Aβ42 (supplementary data, Figure 4S). No difference was found between animals sacrificed 6 or 24 h after the last treatment. In control animals intracellular Aβ was distributed more homogenously within neurons (arrows in E). C, D: Bar 500 µm; E, F: Bar = 50 µm

Figure 7 Altered APP immunostaining in brain after chronic LY-411575 treatment of APP23 mice.

APP23 mice were treated for 3 months with LY-411575. A-D: The C-terminal antibody APP-C8 revealed a reduced staining in neuronal cell bodies compared to vehicle (B, D versus A, C), which was most evident in neocortex layer V (compare A to B, Cx V) and hippocampus (compare C to D). In the CA3 region of the hippocampus, APP-C8 stained mostly neuronal cell bodies in control mice, while nerve fibers were stained in LY-411575 treated animals (insets in C and D). Staining of nerve fibers with APP-C8 was strongly increased in several other brain regions (stratum oriens of CA1, Or; outer and inner neocortical layers, Cx I-II and Cx VI; retrosplenial cortex, RS; subiculum, Sub; mossy fibers, mF; polymorph layer of the dentate gyrus, PoDG; compare A to B). E, F: The reduction of cell body APP staining was also seen with antiserum 474 directed against an epitope in the N-terminus of APP. APP474 did not stain fibers indicating that the fiber staining of APP-C8 represents accumulated C-terminal APP fragments. Boxes in A and B indicate the approximate positions of the higher magnifications shown in C to F. B: Bar = 500 µm (also for A); F: Bar = 50 µm (also for D-E). Large boxes in C to F are insets at higher magnification.

Figure 8 Reduced accumulation of Aβ in brains of plaque bearing APP24 mice during chronic treatment with LY-411575.

Female APP24 mice were treated daily with 3 mg/kg LY-411575 or vehicle for 2 months starting at the age of 15 months, when these mice carry a moderate neocortical amyloid load. Animals (15 per group) were sacrificed at baseline (15 months) and 6 h after the last dose (17 months). A: Aβ1-38, 40 and 42 in forebrain remained at baseline in substance treated mice, while in the vehicle treated group Aβ1-40 and 42 increased as determined by quantitative MALDI-TOF of SDS-extracted and immunoprecipitated Aβ. B: In pons/medulla oblongata, where only very few amyloid plaques are found at 17 months, LY-411575 reduced Aβ1-38 and 1-40 compared to baseline. The increase of Aβ1-42 was only partially inhibited consistent with the formation of early amyloid deposits. Each symbol represents one animal. Lines

JPET Fast Forward. Published on August 7, 2008 as DOI: 10.1124/jpet.108.140327
This article has not been copyedited and formatted. The final version may differ from this version.

indicate the median. Significant differences between groups are indicated by asterisks (Kruskal-Wallis test and Tukey's post hoc test on ranks; $p<0.05$: *; $p=0.01$: **; $p<0.001$: ***).

Figure 9 Reduced plaque formation in brains of APP24 mice with moderate amyloid load during chronic treatment with LY-411575.

APP24 mice were treated from 15 to 17 months with 3 mg/kg LY-411575. A-C: Shown are representative brain sections from a baseline animal at 15 months (A) and from 17 months old treated (B) or vehicle (C) animals. LY-411575 reduced the amyloid deposition. Amyloid plaques were quantified in highlighted regions shown in C (neocortex, Cx and caudate putamen, CPu). C: Bar = 1 mm (also for A and B). D, E: The reduction of amyloid deposition (D: plaque area, E: plaque number) was more pronounced in caudate putamen than in neocortex. Each symbol represents one animal. The lines shows the position of medians. Significant differences are indicated by asterisks (Kruskal-Wallis test and Tukey's post hoc test on ranks; $p<0.05$: *; $p<0.01$: **; $p=0.001$: ***). The amount of inhibition of plaque formation as percent of the difference between baseline and vehicle treated group is indicated.

JPET Fast Forward. Published on August 7, 2008 as DOI: 10.1124/jpet.108.140327
This article has not been copyedited and formatted. The final version may differ from this version.

Table 1: The reduction of amyloid accumulation by chronic γ-secretase inhibition inversely correlates with the initial amyloid load

Line	Treatment	Brain region	Initial plaque area	Efficiency	
			Median	Average	Median
APP23	6-9 mo	neocortex	<0.1%	- 82%	-80%
APP24	15-17 mo	caudate/putamen	0.16%	- 66%	-79%
APP24	15-17 mo	neocortex	1.8%	- 41%	-31%

JPET Fast Forward. Published on August 7, 2008 as DOI: 10.1124/jpet.108.140327
This article has not been copyedited and formatted. The final version may differ from this version.

Figure 1

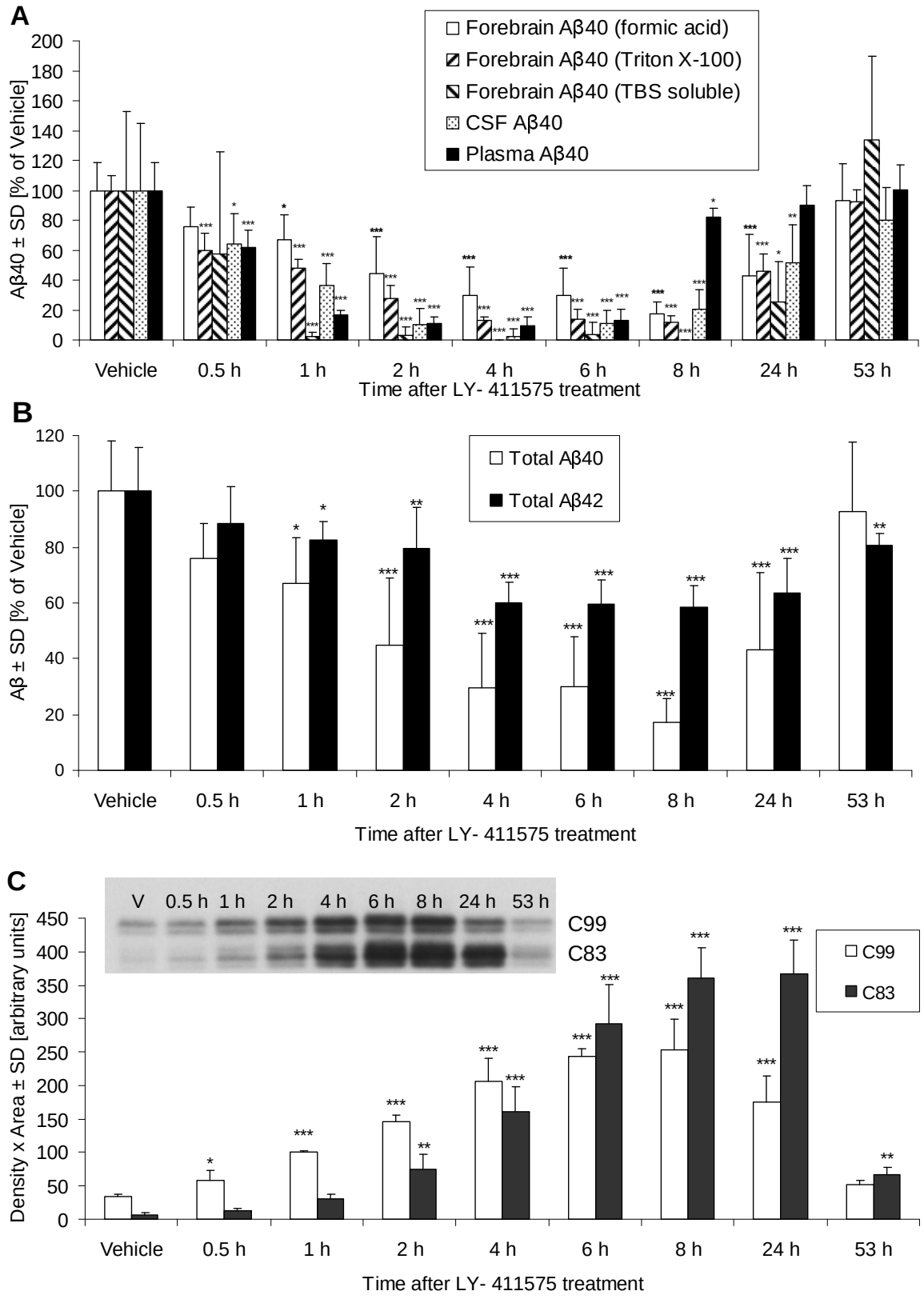

JPET Fast Forward. Published on August 7, 2008 as DOI: 10.1124/jpet.108.140327
This article has not been copyedited and formatted. The final version may differ from this version.

Figure 2

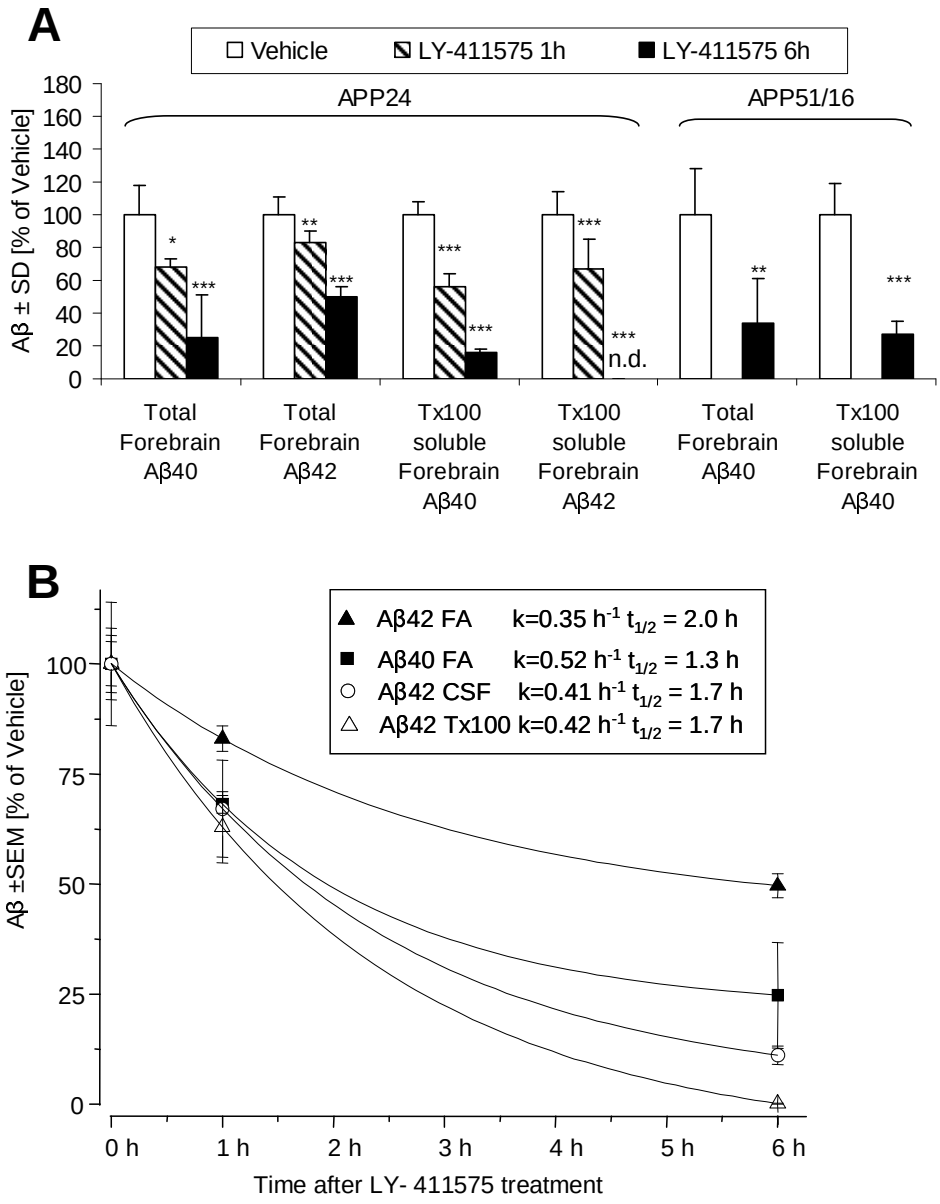

JPET Fast Forward. Published on August 7, 2008 as DOI: 10.1124/jpet.108.140327
This article has not been copyedited and formatted. The final version may differ from this version.

Figure 3

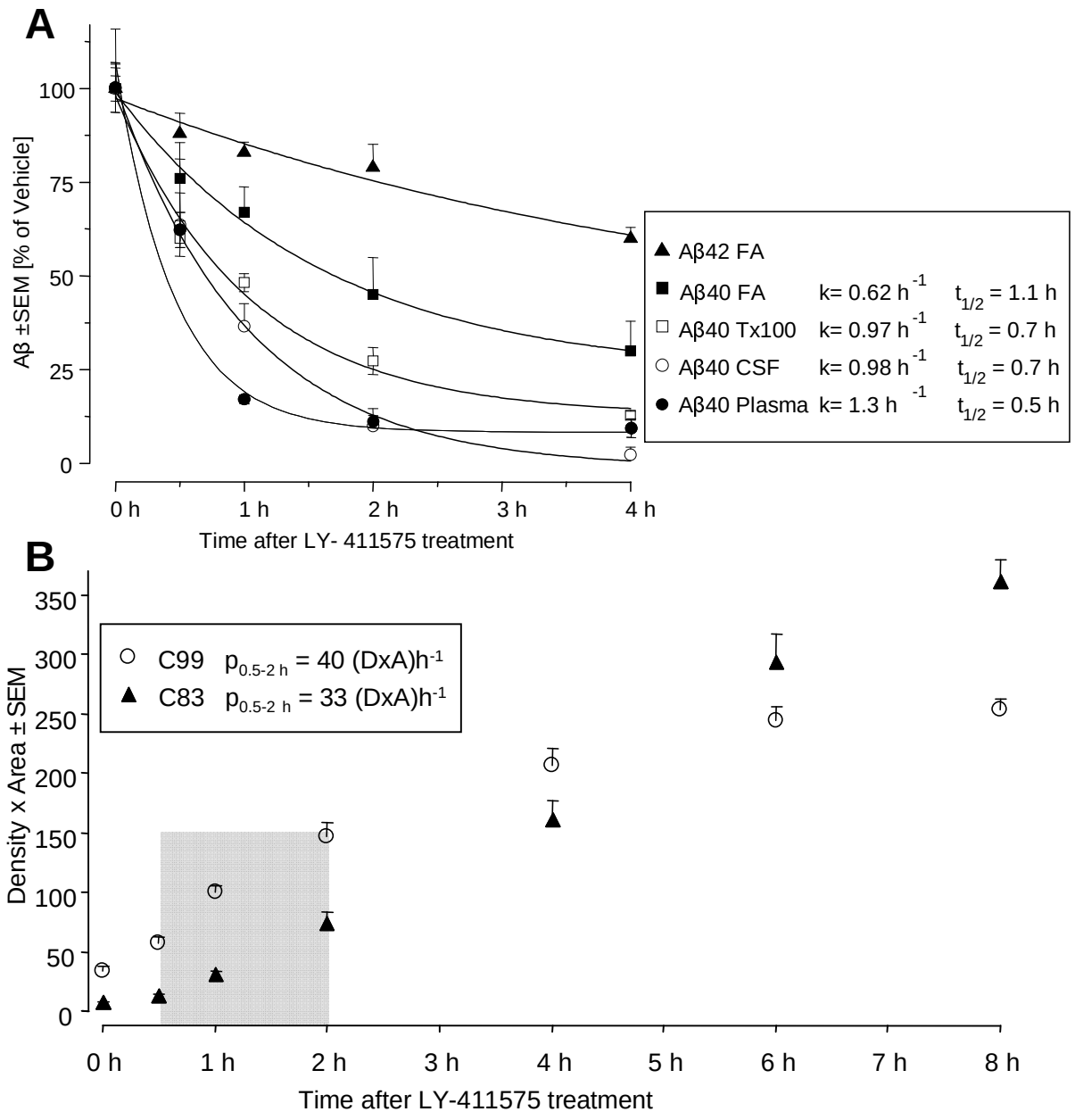

Figure 4

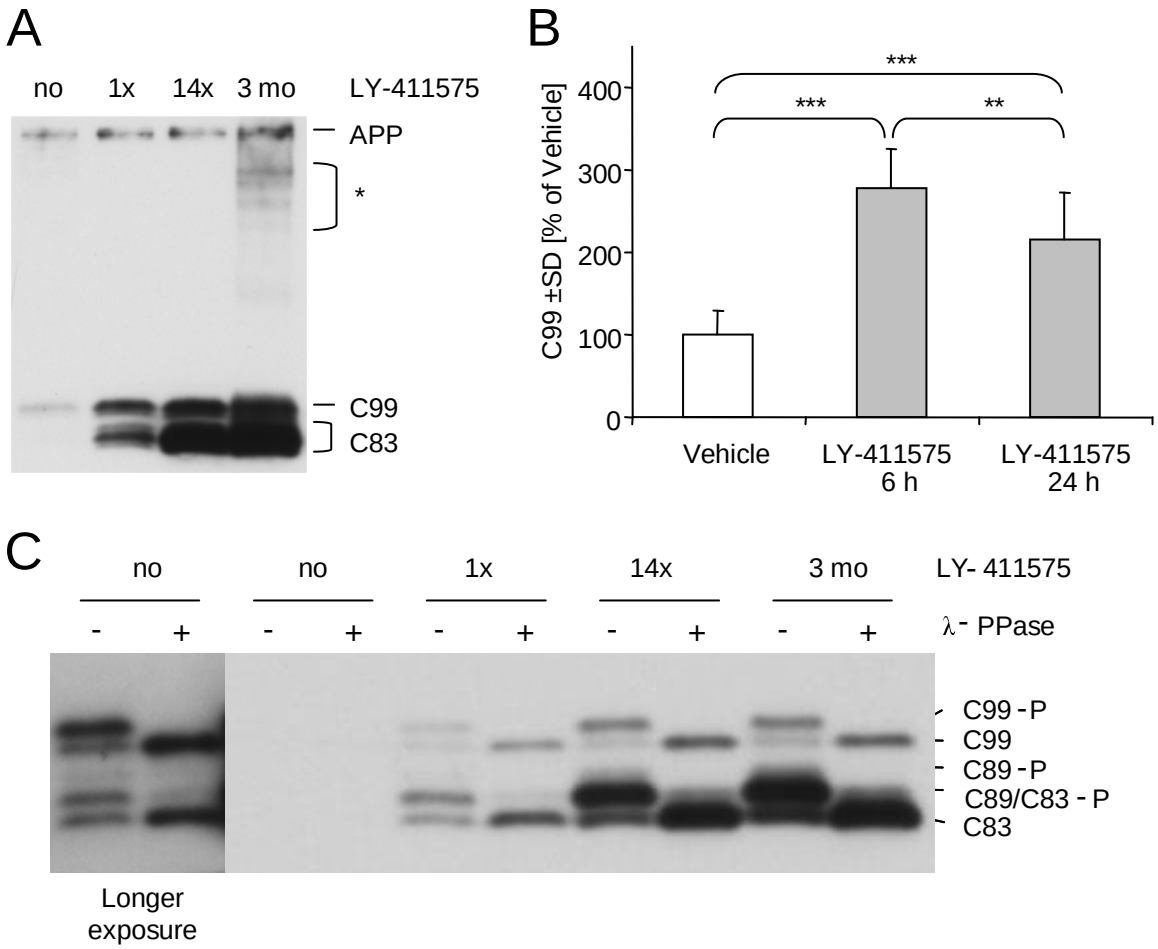

Figure 5

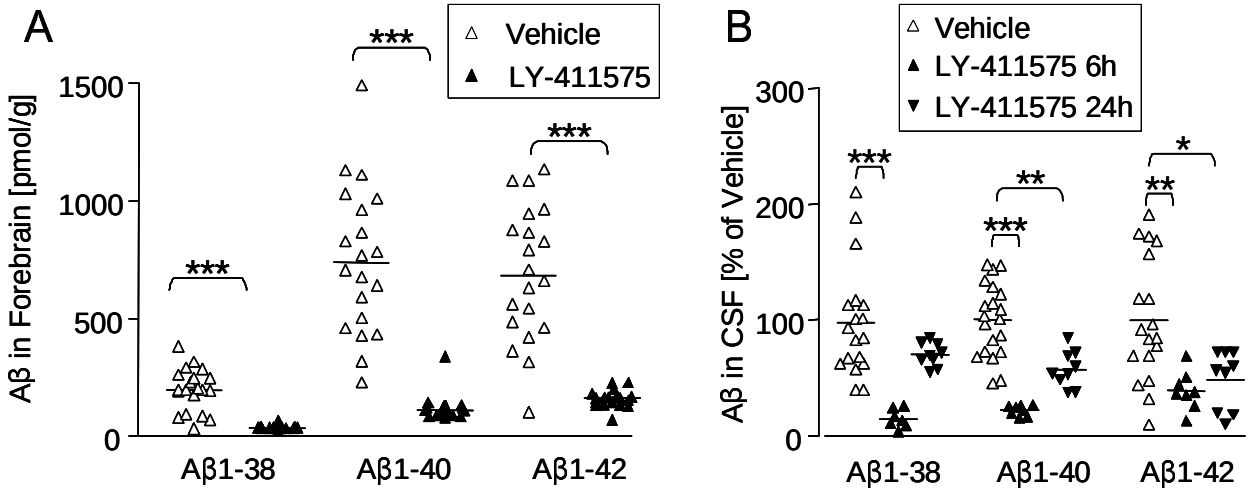

JPET Fast Forward. Published on August 7, 2008 as DOI: 10.1124/jpet.108.140327

Figure 6

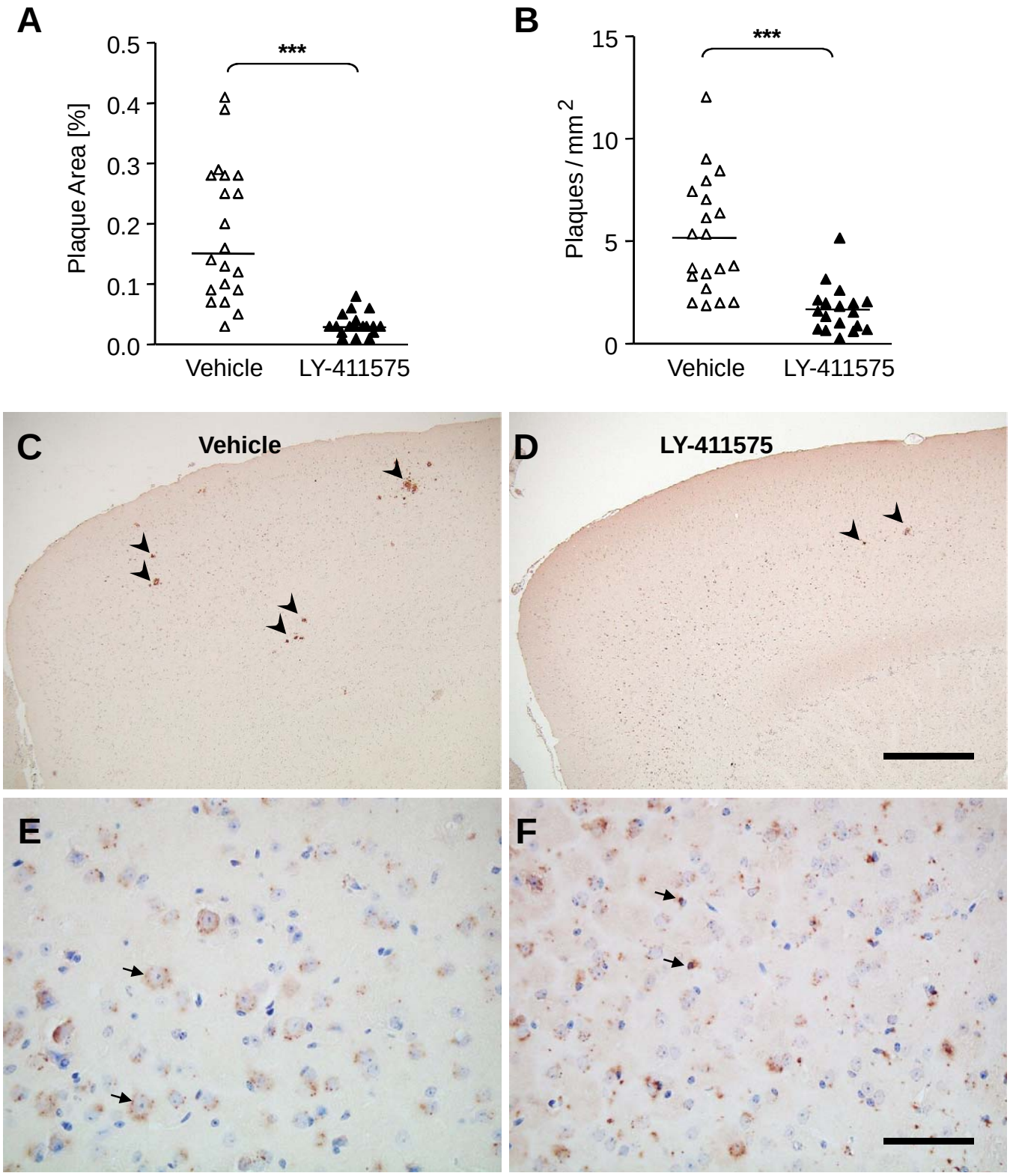

JPET Fast Forward. Published on August 7, 2008 as DOI: 10.1124/jpet.108.140327
This article has not been copyedited and formatted. The final version may differ from this version.

Figure 7

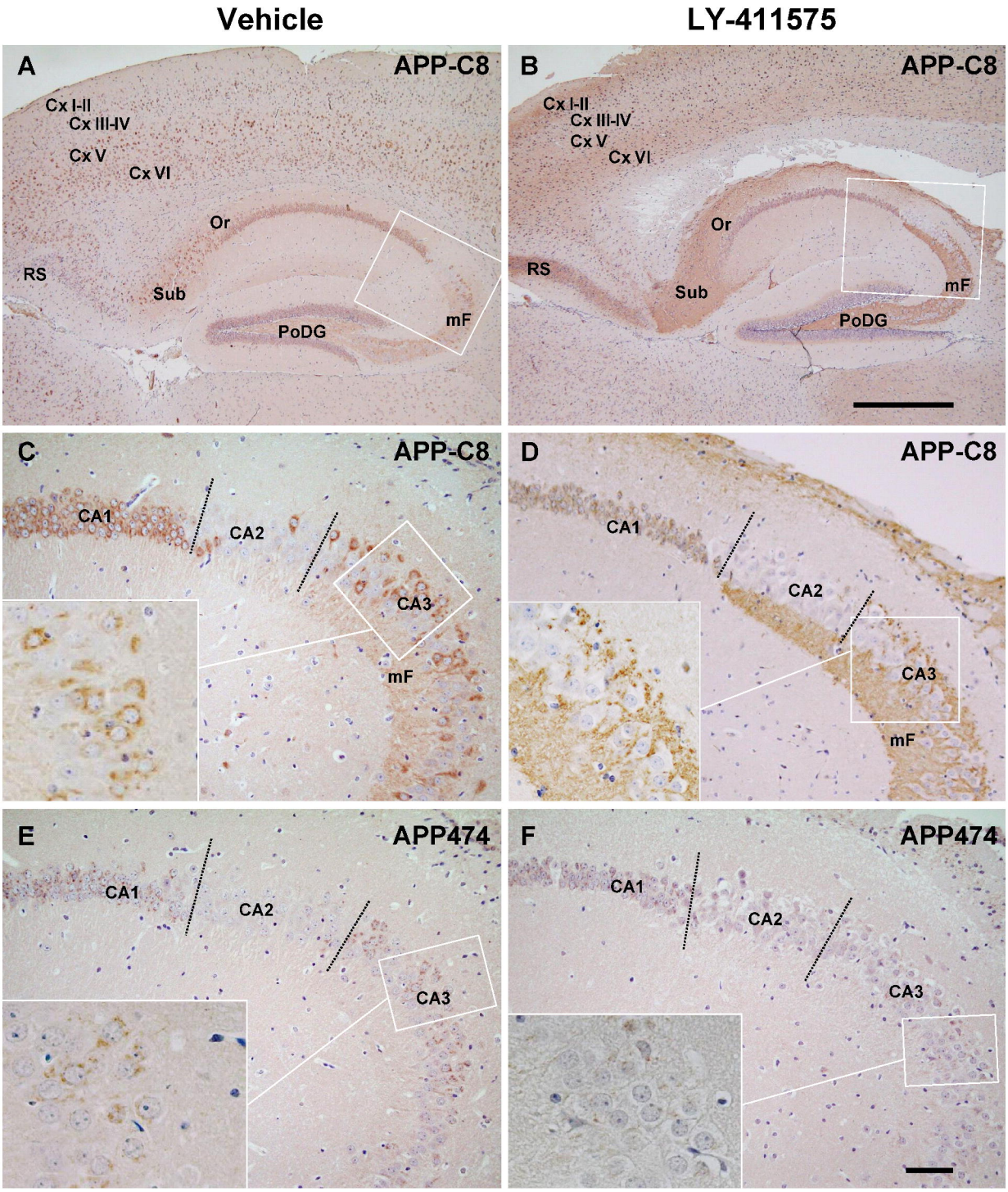

Figure 8

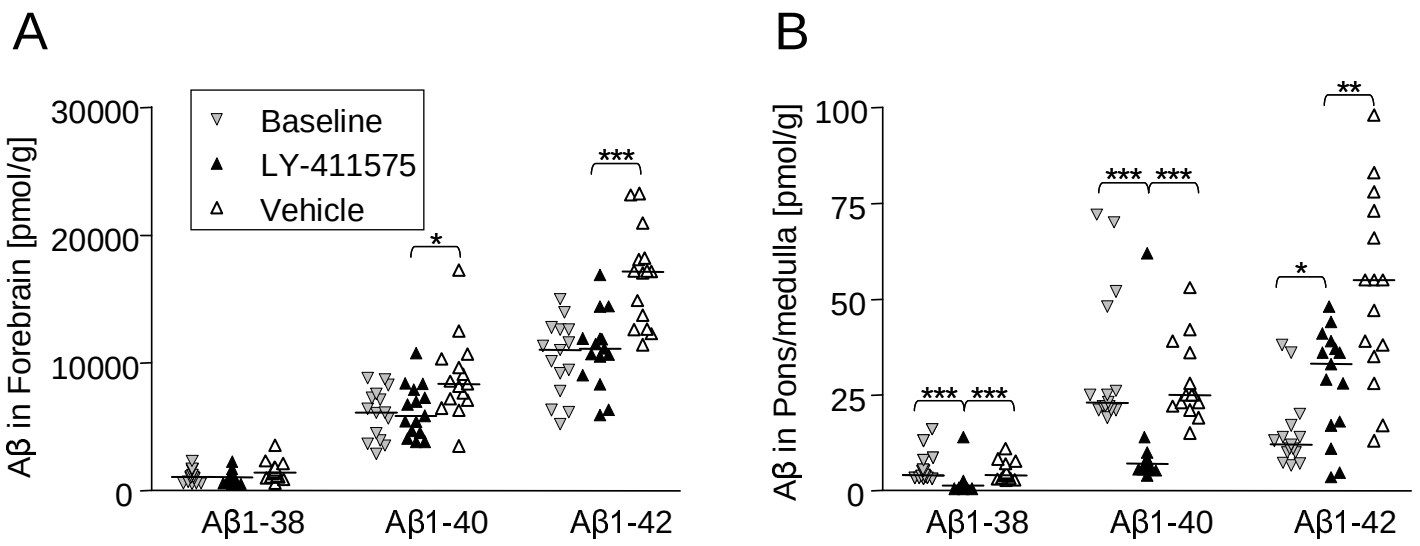

Figure 9